Resolving Intermediate Solution Structures during the Formation of Mesoporous SBA-15

5 **AUTHORS**, INCLUDING:

Sharon Ruthstein
Bar Ilan University

30 PUBLICATIONS **464** CITATIONS

SEE PROFILE

Ellina Kesselman
Technion - Israel Institute of Technology

72 PUBLICATIONS **2,199** CITATIONS

SEE PROFILE

Resolving Intermediate Solution Structures during the Formation of Mesoporous SBA-15

Sharon Ruthstein,[†] Judith Schmidt,[‡] Ellina Kesselman,[‡] Yeshayahu Talmon,[‡] and Daniella Goldfarb*,[†]

Contribution from the Department of Chemical Physics, Weizmann Institute of Science, Rehovot 76100, Israel, and Department of Chemical Engineering, Technion-Israel Institute of Technology, Haifa 32000, Israel

Received August 31, 2005; E-mail: daniella.goldfarb@weizmann.ac.il

Abstract: The evolution of the solution microstructures during the formation of the hexagonal mesoporous material SBA-15 was studied by direct imaging and freeze−fracture replication cryo-TEM. A reaction mixture was sampled at different times after the addition of tetramethoxyorthosilane (TMOS) to an acidic solution of Pluronic P123 held at 50 °C. Solution microstructures were detected by direct imaging cryo-TEM in the time window of 6.5−40 min after the addition of the TMOS ($t = 0$). The micrographs revealed that the initial spheroidal micelles evolve into threadlike micelles, which become longer and straighter with time. Then bundles with the dimensions similar to those found in the final material appeared, although there was no sign of a hexagonal arrangement up to 40 min. Due to the appearance of a precipitate at 40 min the sample became too viscous, preventing clear observation of its content. To observe the structures present after 40 min, freeze−fracture replication was carried out as well. Such samples were collected also at 22 min and showed the presence of threadlike micelles in agreement with the direct imaging cryo-TEM micrographs. The 2 h samples showed some areas of hexagonal ordered structures, which become very clear at 2 h 50 min. The cryo-TEM measurements were carried out under the same reaction conditions used in earlier in situ EPR experiments, thus allowing us to correlate molecular level events with the microstructure shape evolutions. This showed that the elongation of the micelles is a consequence of a reduction of the polarity and the water content within the micelles due to silicate adsorption and polymerization. Similar experiments were carried out also on SBA-15 prepared with HCl and TMOS at 35 °C. The appearance of threadlike micelles, followed by clustering of the TLMs, was observed under these conditions as well, but the reaction rate was faster. This suggests that the observed mechanism for the formation of SBA-15 is general.

Introduction

The discovery of M41S mesoporous materials was a significant breakthrough in the synthesis of open-framework inorganic materials of well-defined geometry.[1,2] The development of such silica composite materials with precise and easily controlled pore shapes and sizes[3−5] is of great importance in many areas of modern science and technology.[6−10] Silica materials exhibiting lamellar, 2D hexagonal, 3D hexagonal, or cubic organizations,

with pore sizes in the range of 1.5−4.0 nm, have been produced with ionic surfactants such as alkyltrimethylammonium bromide.[1,2,11,12] Mesoporous materials with larger pore sizes and better performance in terms of hydrothermal stability were synthesized with nonionic poly(ethyleneoxide)-poly(propyleneoxide)-poly(ethyleneoxide) block copolymer (Pluronics, PEO$_x$-PPO$_y$-PEO$_x$).[13] In these materials the pore diameter can be tuned within the range of 2−30 nm, and a better stability is obtained due to the thicker silica wall (up to 6 nm).[14] SBA-15 has a hexagonal structure and is prepared with Pluronic P123 (PEO$_{20}$PPO$_{70}$PEO$_{20}$), while SBA-16 is cubic and is synthesized with Pluronic F127 (PEO$_{106}$PPO$_{70}$PEO$_{106}$).[13,15] Compared to ionic surfactants, block copolymers have become more and more popular in the synthesis of mesoporous solids, because of their diverse structural characteristic, rich phase behavior, low cost,

† Weizmann Institute of Science.
‡ Technion-Israel Institute of Technology.
(1) Beck, J. S.; Vartuli, J. C.; Roth, W. J.; Lenowicz, M. E.; Kresge, C. T.; Schmidt, K. D.; Chu, C. T.-W.; Olson, D. H.; Sheppard, E. W.; McCullen, S. B.; Higgins, J. B.; Schlenker, J. L. *J. Am. Chem. Soc.* **1992**, *114*, 10834.
(2) Kresge, C. T.; Leonowicz, M. E.; Roth, W. J.; Vartuli, J. C.; Beck, J. S. *Nature* **1992**, *359*, 710.
(3) Ciesla, U.; Schüth, F. *Microporous and Mesoporous Materials* **1999**, *27*, 131.
(4) Selvam, P.; Bhatia, S. K.; Sonwane, C. G. *Ind. Eng. Chem. Res.* **2001**, *40*, 3237.
(5) Davidson, A. *Curr. Opin. Colloid Interface Sci.* **2002**, *7*, 92.
(6) Corma, A. *Chem. Rev.* **1997**, *97*, 2373.
(7) Moller, K.; Bein, T. *Chem. Mater*. **1998**, *10*, 2950.
(8) Wu, C. G.; Bein, T. *Science* **1994**, *264*, 1013.
(9) Diaz, J. F.; Balkus, K. J. *J. Mol. Catal. B: Enzym.* **1996**, *2*, 115.
(10) Wirnsberger, G.; Yang, P.; Scott, B. J.; Chmelka, B.; Stucky, G. D. *Spectrochimica Acta, Part A* **2001**, *57*, 2049.

(11) Huo, Q.; Leon, R.; Petroff, P. M.; Stucky, G. D. *Science* **1995**, *268*, 1324.
(12) Zhao, D.; Goldfarb, D. *J. Chem. Soc., Chem. Commun*. **1995**, 875.
(13) Zhao, D.; Huo, Q.; Feng, J.; Chmelka, B. F.; Stucky, G. D. *J. Am. Chem. Soc.* **1998**, *120*, 6024.
(14) Zhao, D.; Feng, J.; Huo, Q.; Melosh, N.; Fredrickson, G.; Chmelka, B. F.; Stucky, G. D. *Science* **1998**, *279*, 548.
(15) Van de Voort, P.; Benjelloun, M.; Vansant, E. F. *J. Phys. Chem. B* **2002**, *106*, 9027.

and nontoxic degradation.[16,17] Different synthesis methodologies have been developed, carefully manipulating reaction parameters such as temperature, pH, ionic strength, reaction time, and solution composition.[18,19]

The formation process of mesoporous materials is fascinating. The synthesis mixture contains four major components: inorganic precursors, organic template molecules, solvent, and acid/base catalyst. The formation of a material with a desired structure and morphology depends on a delicate interplay between several basic processes, whose relative rates determine the structure and properties of the final structure. These are the self-assembly of the organic molecules to form structures that serve as templates, the sol−gel chemistry that generates the inorganic network, and the specific interaction at the interface between the organic assemblies and the forming inorganic oligomers.[19] There are different models to describe how the inorganic phase interacts with the organic surfactant molecules.[20,21] Beck et al.[1] suggested the "liquid-crystal templating" (LCT) mechanism soon after the discovery of MCM-41. They proposed two main general pathways, in which either (i) the liquid-crystal phase pre-exists before the silicate species are added or (ii) the addition of the silicate anions promotes the long range ordering of the surfactant to form the hexagonal arrangement. Firouzi et al.[22] reported experimental evidence for pathway (ii) for MCM-41 and showed through ^{2}H and ^{29}Si NMR spectroscopy, as well as neutron scattering, that a micellar solution of cetyltrimethylammonium bromide (CTAB) transformed into a hexagonal lyotropic phase in the presence of silicate anions. Pathway (ii) has been referred to as the cooperative self-assembly mechanism (CSA).

In principle the reaction mechanism can be viewed at three length scales: (i) the molecular one, which concentrates on the interaction between the organic and inorganic precursors and on the silica polymerization process; (ii) the mesoscopic scale, which involves the development of the micellar structures and the onset of the long-range order; and finally (iii) the macroscale which is related to the shape/morphology of the final product. It is clear that the changes that occur at the molecular level are the driving force for the mesoscale structure, but the question is how the two scales are correlated. So far, most of the in situ mechanistic studies concentrated on molecular level observations using spectroscopic techniques such as EPR, NMR, and IR.[23−33] In addition, a number of in situ small-angle X-ray scattering

(SAXS) studies targeting the mesoscale have been reported.[34,35] Yet, there is no clear correlation between them, because most of the studies were carried out on different systems and under different conditions. Recently, the development of the morphology of the particles with time (ex situ) and its dependence on the reaction conditions were used to suggest a colloidal-like phase separation mechanism for the formation of SBA-15.[36]

We introduced the use of in situ continuous wave (CW) EPR and freeze−quench electron-spin−echo envelope modulation (ESEEM) spectroscopy of spin probes as efficient methods for investigating the formation mechanism of mesostructured materials on the molecular level,[29] which was applied to MCM-41 and SBA-15.[30−33] Ottaviani and co-workers have also extensively used CW EPR.[37] In these experiments information regarding changes in the tumbling rate of the organic molecules, in the polarity and in the water content of their close environment during the reaction, was obtained. Here, we sought further insight into the formation of SBA-15, focusing on the structure evolution on the mesoscopic scale. Hence we applied cryogenic-TEM (cryo-TEM) carried out under the same reaction conditions as the EPR experiments, to allow the correlation between the two length scales. In cryo-TEM the supramolecular structures in solution are observed by vitrifying a thin layer of a solution without staining or drying the sample, which may change the properties of the intermediates. Cryo-TEM is a powerful tool for investigating nanostructures in soft materials. It has been applied to image micelles formed by conventional surfactants as well as block copolymers.[38,39] Earlier cryo-TEM on reaction mixtures of MCM-41 reported a single time point snapshot, showing the formation of ellogonated micelles and vesicles during the synthesis of MCM-41 in the presence of decanoate.[40] Time-resolved TEM measurements combined with in situ ^{1}H NMR were also carried out on the reaction mixture of SBA-15.[26] There, the reaction was quenched by dilution and a pH change, and specimens of the intermediates structure were retrieved by drying. The last two steps, however, may affect the solution structures.

Here we present a sequence of cryo-TEM "snapshots" of the formation of SBA-15, which show the evolution of the solution structures and their average diameters up to the formation of a thick precipitate, prior to the formation of the hexagonal structure. The final hexagonal structure was observed in freeze fracture replication. These results provide new insight into the formation mechanism along with clear experimental evidence for some of its essential steps.

(16) Booth, C.; Attwood, D. *Macromol. Rapid Commun.* **2000**, *21*, 501.
(17) Alexandridis, P.; Hatton, T. A. *Colloids and Surfaces, A: Physicochemical and Engineering Aspects* **1995**, *96*, 1.
(18) Soler-Illia, G. J. de A. A.; Sanchez, C.; Lebeau, B.; Patarin, J. *Chem. Rev.* **2002**, *102*, 4093.
(19) Soler-Illia, G. J. de A. A.; Crepaldi, E. L.; Grosso, D.; Sanchez, C. *Curr. Opin. Colloid Interface Sci.* **2003**, *8*, 109.
(20) Ying, J. Y.; Mehnert, C. P.; Wong, M. S. *Angew. Chem., Ind. Ed.* **1999**, *38*, 56.
(21) Patarin, J.; Lebeau, B.; Zana, R. *Curr. Opin. Colloids Interface Sci.* **2002**, *7*, 107.
(22) Firouzi, A.; Kumar, D.; Bull, L. M.; Besier, T.; Sieger, P.; Huo, Q.; Walker, S. A.; Zasadzinski, J. A.; Glinka, C.; Nicol, J.; Margolese, D.; Stucky, G. D.; Chmelka, B. F. *Science* **1995**, *267*, 1138.
(23) Caldararu, H.; Caragheorgheopol, A.; Savonea, F.; Macquarrie, D. J.; Gilbert, B. C. *J. Phys. Chem. B* **2003**, *107*, 6032.
(24) Galarneau, A.; Renzo, F. D.; Fajula, F.; Mollo, L.; Fubini, B.; Ottaviani, M. F. *J. Colloid Interface Sci.* **1998**, *201*, 105.
(25) Fresch, J.; Lebeau, B.; Soluard, M.; Patarin, J.; Zana, R. *Langmuir* **2000**, *16*, 9049.
(26) Flodström, K.; Wennerström, H.; Alfredsson, V. *Langmuir* **2004**, *20*, 680.
(27) Holmes, S. M.; Zholobenko, V. L.; Thursfield, A.; Plaisted, R. J.; Cundy, C. S.; Dwyer, J. *J. Chem. Soc., Faraday Trans.* **1998**, *94*, 2025.
(28) Calabro, D. C.; Valyocsik, E. W.; Ryan, F. X. *Microporous Materials* **1996**, *7*, 243.
(29) Zhang, J.; Luz, Z.; Goldfarb, D. *J. Phys. Chem. B* **1997**, *101*, 7087.
(30) Zhang, J.; Luz, Z.; Zimmermann, H.; Goldfarb, D. *J. Phys. Chem. B* **2000**, *104*, 279.
(31) Zhang, J.; Carl, P. J.; Zimmermann, H.; Goldfarb, D. *J. Phys. Chem. B* **2002**, *106*, 5382.
(32) Ruthstein, S.; Frydman, V.; Kababya, S.; Landau, M.; Goldfarb, D. *J. Phys. Chem. B* **2003**, *107*, 1739.
(33) Ruthstein, S.; Frydman, V.; Goldfarb, D. *J. Phys. Chem. B* **2004**, *108*, 9016.
(34) Lindén, M.; Schunk, S. A.; Schüth, F. *Angew. Chem., Int. Ed.* **1998**, *37*, 6, 821.
(35) Flodström, K.; Teixeira, C. V.; Amenitsch, H.; Alfredsson, V.; Lindén, M. *Langmuir* **2004**, *20*, 4885.
(36) Yu, C.; Fan, J.; Tian, B.; Zhao, D. *Chem. Mater.* **2004**, *16*, 889.
(37) Ottaviani, M. F.; Moscatelli, A.; Desplantier-Giscard, D.; Di Renzo, F.; Kooyman, P. J.; Alonso, B.; Galarneau, A. *J. Phys. Chem. B* **2004**, *108*, 12123.
(38) Bernheim-Groswasser, A.; Wachtel, E.; Talmon, Y. *Langmuir* **2000**, *16*, 4131.
(39) Nilsson, S.; Goldraich, M.; Lindman, B.; Talmon, Y. *Langmuir* **2000**, *16*, 6825.
(40) Pevzner, S.; Regev, O.; Lind, A.; Lindèn, M. *J. Am. Chem. Soc.* **2003**, *125*, 652.

Experimental Section

Synthesis. The reagents used for the synthesis were as follows: Pluronic P123 ($PEO_{20}PPO_{70}PEO_{20}$) average molecular weight, M_{av}, of 5800, a gift from BASF Corp. (USA); tetramethoxy orthosiliane ($(CH_3O)_4Si$, TMOS, 98% pure, Merck); orthophosphoric acid (85% H_3PO_4, Fluka).

SBA-15 was synthesized according to the procedure reported by Zhao et al.,[41] except for the replacement of hydrochloric acid (HCl) by orthophosphoric acid (H_3PO_4).[32,42] A typical SBA-15 synthesis was as follows: to 16 mL of aqueous solution held at 50 °C containing 0.5 g of P123 (86.2 μmol), 1.2 mL (12 mmol) of H_3PO_4 (85%) was added, and the mixture was stirred for 2 min, followed by the addition of 0.8 mL (5 mmol) of TMOS. The resulting mixture was left under stirring conditions for 20 h at 50 °C and then transferred into a Teflon bottle and heated at 100 °C for 24 h without stirring. After cooling to room temperature, the solid product was recovered by filtration, washed with distilled water, and dried in air at ambient temperature. A typical molar composition of the synthesis gel was as follows: TMOS: 1.7×10^{-2} P123: 2.4 H_3PO_4: 175 H_2O. For comparison, SBA-15 was also prepared under Zhao's[41] conditions, carried out at 35 °C with HCl and the molar ratio of reaction mixture was as follows: TMOS: 1.7×10^{-2} P123: 4.75 HCl: 175 H_2O.
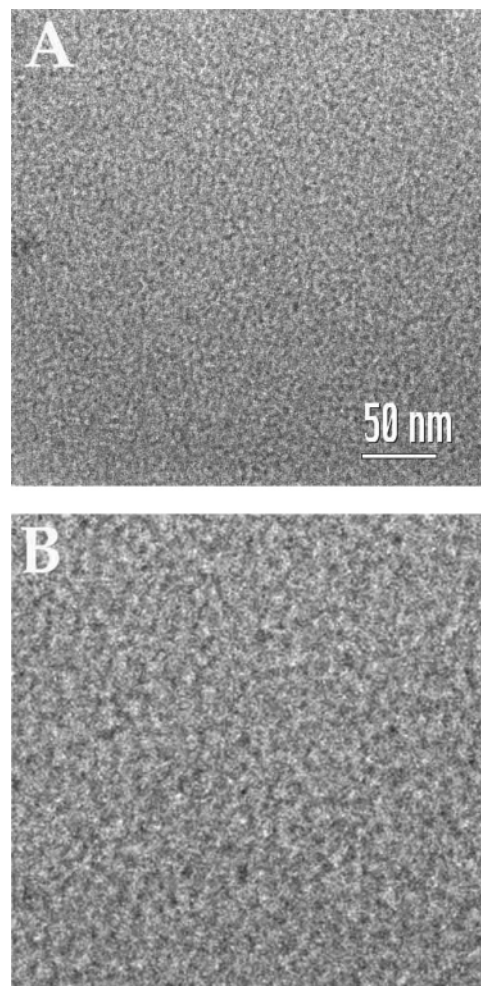
The final product was characterized by small-angle X-ray scattering (SAXS), using a diffractometer equipped with a Franks mirror and a one-dimensional position-sensitive detector (homemade), using nickel-filtered Cu Kα radiation ($\lambda = 1.54$ Å). All final products exhibited SAXS patterns of well-ordered SBA-15.[32]

Methods. Vitrified specimens for cryo-TEM were prepared in a controlled environment vitrification system (CEVS).[43] All solutions were quenched from 50 °C and 100% relative humidity by plunging into liquid ethane at its melting point. Specimens were examined in a Philips CM120 microscope, operated at 120 kV, using an Oxford CT-3500 cryo-holder system. All specimens were observed in the microscope below −178 °C. Images were recorded digitally in the minimal electron dose mode by a Gatan 791 MultiScan CCD camera with the DigitalMicrograph software package.

Freeze−fracture replication (FFR) was performed with a BAF-060 system (BalTech AG, Liechtenstein). A small drop of the sample was placed between two electron microscopy copper grids, and those were sandwiched between two gold planchettes. The "sandwich" was plunged into liquid ethane at its freezing point, transferred into liquid nitrogen, and inserted into a sample fracture block, precooled in liquid nitrogen. The block was inserted into the BAF-system vacuum chamber, maintained at −160 °C to −170 °C, and was split open to fracture the frozen sample drop. The fracture surfaces were first shadowed at a 45° angle with a 2 nm layer of platinum−carbon, followed by backing with a 20 nm thick carbon layer. The replicas were retrieved from the thawed samples, cleaned in double-distilled water, mounted on TEM grids, and examined in the Philips CM120 or FEI T12 TEMs (see above) at room temperature.

Results

The microstructures formed in the solution were explored by sampling the reaction mixture of SBA-15, held at 50 °C, as a function of time. The synthesis procedure was similar to that described in our earlier publications,[32,33] where HCl has been replaced with phosphoric acid to minimize the decomposition of the spin label used in the EPR measurements. The final material obtained using this procedure was highly ordered as shown by the standard characterization techniques.[32] We used

(41) Zhao, D.; Sun, J.; Li, Q.; Stucky, G. D. *Chem. Mater.* **2000**, *12*, 275.
(42) Rozantsev, E. G. *Free Nitroxyl Radicals*; Plenum Press: New York, London, 1970.
(43) Talmon, Y. In *Modern Characterization Methods of Surfactants Systems*; Binks, B. P., Ed.; Modern Dekker: New York, 1999; p 147.

Figure 1. (A) Cryo-TEM image of spheroidal micelles found in the reaction mixture of SBA-15, taken after a reaction time of 8.5 min, vitrified from 50 °C. (B) Same area at double the magnification of A.

the same reaction conditions to allow correlation of the cryo-TEM results with those of the earlier EPR measurements. Under our reaction conditions the solution became turbid after 20 min, and a precipitate appeared at ~40 min.

The time limit of the direct imaging cryo-TEM experiments was 40 min, because at longer times the prepared specimens became too thick, preventing the detection of clear structures. Only dilute regions of micellar solution were observed at longer times. In addition, no structures could be detected prior to the addition of the TMOS ($t = 0$) nor for a sample taken at $t = 1.5$ min, although it is known that at the P123 concentration and temperature used micelles are present.[32,44] This is attributed to the low electron density of P123.[45]

At $t = 6.5-8.5$ min spheroidal micelles became detectable as shown in Figure 1 for $t = 8.5$ min. The exact size of the micelles, however, could not be evaluated due to overlap of micelles. At $t = 22$ min flexible threadlike micelles (TLMs), denoted by arrows in Figure 2B, coexist with spheroidal micelles (Figure 2A). At this time, the average diameter of the spheroidal micelles is 9.7 ± 1 nm, while that of the TLMs is 7.1 ± 0.9 nm and their lengths vary between 15 and 30 nm (Figure 2B). At $t = 22-30$ min the diameter of these micelles decreases

(44) Wanka, G.; Hoffman, H.; Ulbricht, W. *Macromolecules* **1994**, *27*, 4145.
(45) Mortensen, K.; Talmon, Y.; Gao, B.; Kops, J. *Macromolecules* **1997**, *30*, 6764.
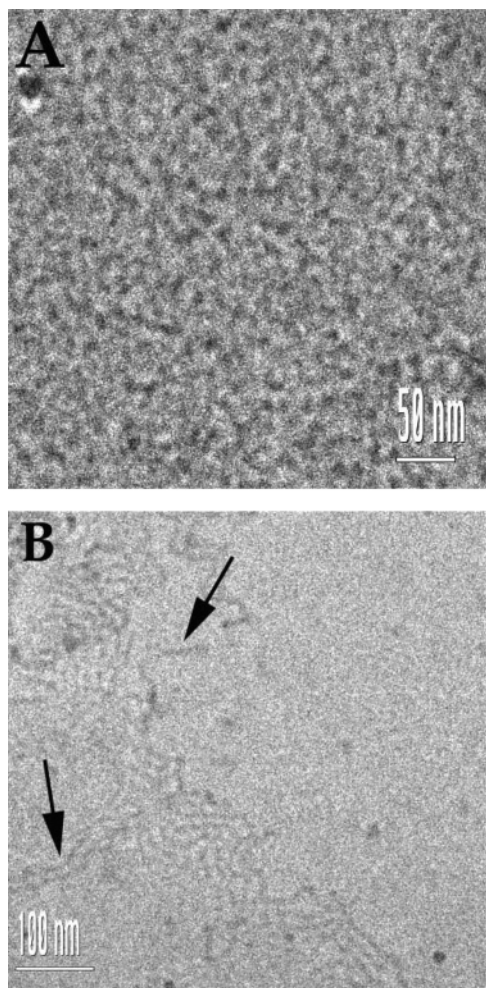
Figure 2. Cryo-TEM images of spheroidal micelles (A) and threadlike micelles (arrows in 2B) in the reaction mixture of SBA-15, taken after 22 min.

slightly. For example, at $t = 25$ min, their average diameter is 5.9 ± 0.7 nm, whereas, at $t = 27$ min, is 5.8 ± 0.6 nm. At $t = 30$ min (Figure 3A), the density of the TLMs increases, their length grows to the range $30-100$ nm and aggregates become apparent. In addition, the diameter of the coexisting spheroidal micelles has now decreased significantly to 4.4 ± 0.9 nm. Later, at $t = 33$ min, the TLMs become less flexible and some short-range organization is formed (Figure 3B−3D). Now the diameter of the TLMs is 6.2 ± 0.8 nm, and their length can exceed 700 nm. Within the bundles the distance between individual TLMs is 11 ± 0.7 nm. A few minutes later, at $t = 40$ min (Figure 4), these structures grow and form a network of threads with a diameter of 5.1 ± 0.5 nm and a spacing of 10.7 ± 1.7 nm. Nitrogen absorption measurements showed that the pore diameter of the final mesoporous material is ∼4 nm, and the 100 d spacing is ∼10.8 nm.[32] These numbers are very close to what was observed by cryo-TEM at 40 min. Although the network at $t = 40$ min (Figure 4) does not give a good diffraction pattern yet, it may be a precursor of the final hexagonal structure. At times longer than 40 min, the sample comprised thick regions, with no resolved structure, coexisting with diluted regions that are characterized by micellar solution. Table 1 summarizes the structures detected by direct imaging cryo-TEM and their sizes. At all times spheroidal micelles were observed, and a consistent decrease in their diameter was noted.

In the case of the TLMs, an initial increase in their diameter was followed by a decrease, and a continuous elongation was observed

The procedure used to prepare specimens for cryo-TEM can affect the microstructure of the systems, due to the shearing of the solution during blotting.[46,47] Shear, for example, can induce alignment of threadlike micelles, to cause a transition from threadlike micelles into vesicles, or threadlike micelles can become strongly entangled. This phenomenon is mostly observed in systems where a phase transition occurred, as in our case. To ensure that this does not happen in our system, several samples were taken, at repeated times, and freeze−fracture replication (FFR) was applied, particularly for $t \geq 40$ min, where direct imaging cryo-TEM is not practical. The results obtained are consistent with those of the direct-imaging cryo-TEM images. At $t = 30$ and 40 min of reaction, the solution is characterized as a bulk solution with TLMs (Figure 5A,B). At 2 h and 50 min (Figure 5C,D), the hexagonal nature of the structure becomes very clear: a black arrow in Figure 5C points to TLMs imaged perpendicularly to their long axis, showing a series of parallel lines; white arrows in Figure 5C and 5D point to TLMs imaged parallel to their long axis, showing their hexagonal arrangement in the bundle, with a d spacing of 14 ± 6 nm. One should keep in mind that those are images of replicas of fracture surfaces of the thermally fixed samples. Different areas may fracture differently, thus showing different views of the same phase. In direct imaging (Figures 1−4) the entire sample is projected on the camera detector due to the very large depth of field of the TEM.

To verify that the evolution of the micellar structures observed in solution is a general feature of the formation mechanism of SBA-15, we carried out similar cryo-TEM measurements on a SBA-15 formed under the more standard conditions. In this synthesis, HCl was used instead of H_3PO_4, and the temperature was 35 °C. Due to the more acidic conditions (pH < 1), the condensation of the silica was faster and reduced the precipitation time to 18 min, as opposed to 40 min in the previous conditions. Therefore, direct-imaging cryo-TEM specimens could be observed until the precipitation time, and at longer times FFR was used to identify the microstructures. In Figure 6A we present a direct-imaging cryo-TEM micrograph of the system after a short reaction time of 5 min 13 sec. The structure is that of spheroidal micelles. Due to the relatively high concentration the projection of several layers of micelles on the TEM detector are actually observed. After 14 min 5 sec the same technique shows TLMs (arrows in Figure 6B). As is quite common in such images of TLMs, especially at relatively high concentration, the micelles are aligned in some areas by the flow during specimen preparation, while in other areas one sees the projection of randomly oriented TLMs. Freeze−fracture replication of the system at about the same time of 16 min 27 sec (Figure 6C) also shows the TLMs (arrows). At 21 min 42 sec, Figure 6D, FFR reveals the hexagonal arrangement of the TLMs. Note the hexagonal arrangement of the micelles seen along their long axes (arrowhead) and the view perpendicular to the long axis (arrow). While the spacings at 21 min 42 sec are very uniform,

(46) Danino, D.; Talmon, Y.; Zana, R. *Colloids and Surfaces, A: Physicochemical and Engineering Aspects* **2000**, *169*, 67.
(47) Zheng, Y.; Lin, Z.; Zakin, J. L.; Talmon, Y.; Davis, H. T.; Scriven, L. E. *J. Phys. Chem. B* **2000**, *104*, 5263.
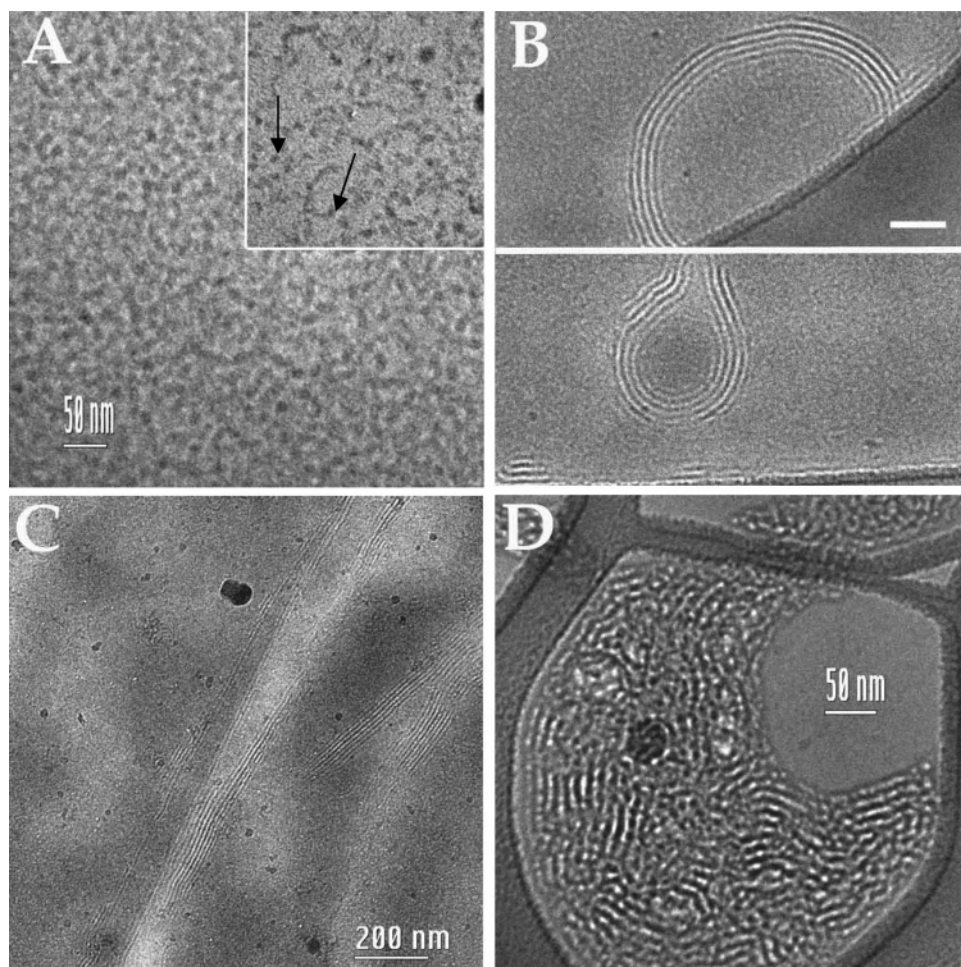
Figure 3. Threadlike micelles found in 50 °C reaction mixture of SBA-15, recorded by cryo-TEM after a reaction time of (A) 30 min and (B−D) 33 min. Images A and B are of the same magnification. The inset in Figure 3A shows an area in the middle right of the main panel, at double the magnification. The arrows point to TLMs.
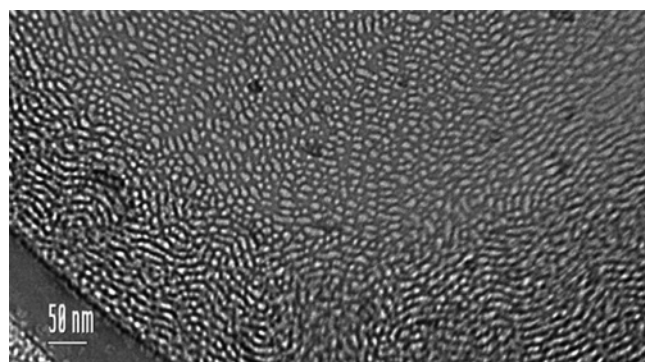
Figure 4. A cryo-TEM image of a network of threadlike micelles in the reaction mixture of SBA-15, taken after a reaction time of 40 min, vitrified from 50 °C.

the nonuniform spacings between the TLMs in Figure 6C (16 min 27 sec) indicate that those are, indeed, free TLMs.

Discussion

Time-resolved cryo-TEM study of the formation of SBA-15 using H_3PO_4 or HCl revealed essentially the same process, with the difference that with HCl the process is much faster and, therefore, less easily resolved. The H_3PO_4 reaction was slow enough and clearly revealed the following process: upon the addition of TMOS the initial spheroidal micelles transformed

Table 1. Summary of the Shapes and Sizes of the Structures Observed during the Formation of SBA-15 with H_3PO_4

time, min	diameter of spheroidal micelles, nm	diameter of TLMs, nm	length of TLMs, nm	spacing, nm
22	9.7 ± 1	7.1 ± 0.9	15−30	
25	5.9 ± 0.7	6.8 ± 1.5	max 400	10 ± 2
27	5.8 ± 0.6			
30		8.4 ± 0.9	30−100	
31	4.4 ± 0.9			
33		6.2 ± 0.8	300−700	11 ± 0.7
40		5.1 ± 0.5		10.7 ± 1.7
90[a]	4.0 ± 1.2			
133[a]	3.5 ± 1.1			

[a] Micelles in the diluted phase.

into elongated micelles with lengths of 15−30 nm, which further developed into TLMs of up to 700 nm long. The TLMs can be straight or curved and may appear as individual entities or as bundles. All this happens prior to the formation of the ordered hexagonal structure, which occurred around 2−3 h, as observed by FFR. In addition, the micrographs of all samples collected between 20 and 40 min show the presence of spheroidal micelles. This is an indication to the presence of two phases in the solution: a more concentrated one in which the TLMs develop and a second dilute one, consisting of spheroidal micelles. This has been also observed in in situ SAXS/XRD
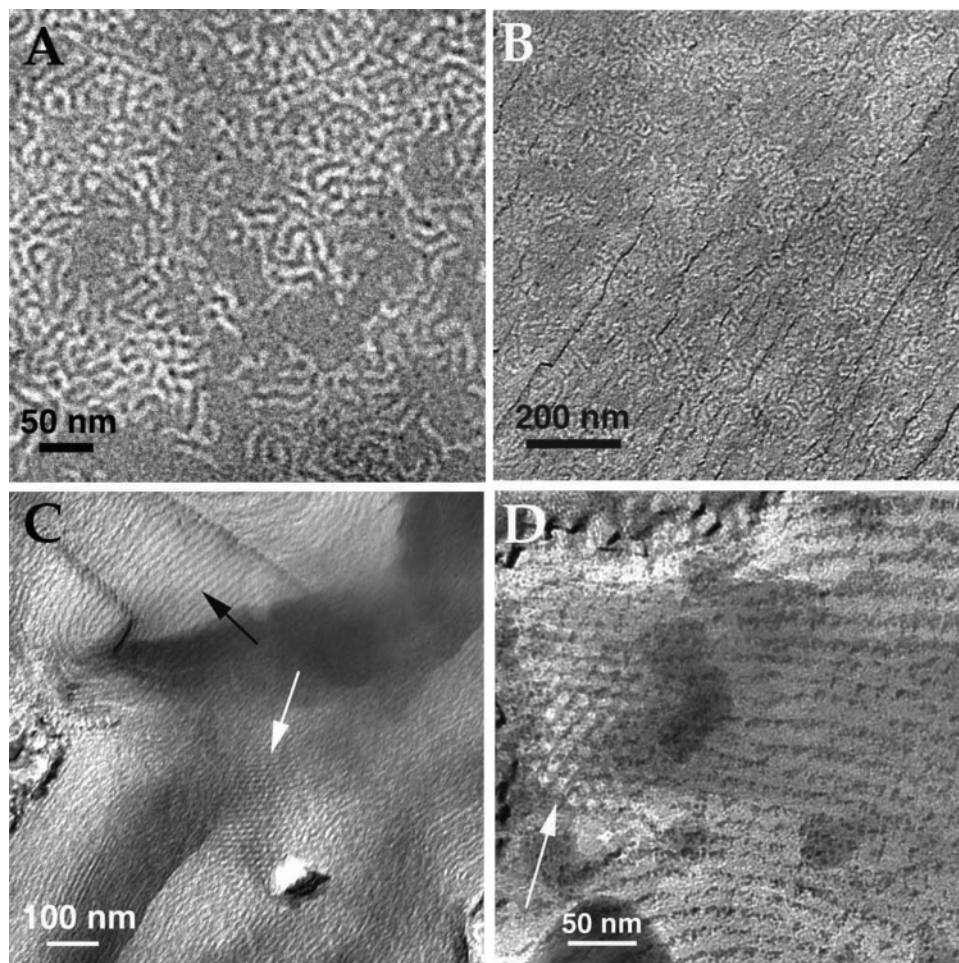
Figure 5. Micrographs of freeze−fracture replicas prepared after an SBA-15 50 °C reaction time of (A) 30 min, (B) 40 min, and (C and D) 2 h and 50 min. Black arrow in image C points to TLMs imaged perpendicularly to their long axis; white arrows in images C and D point to TLMs imaged parallel to their long axis, showing their hexagonal arrangement in the bundle.

studies of SBA-15 prepared under somewhat different conditions.[35]

Comparison with EPR Results. Due to the low electron density of P123[45] spheroidal micelles were not observed in the P123 solution and also 1.5 min after the addition of TMOS. This is in contrast to micelles of 1 wt % poly(ethyleneoxide-*b*-butadiene) (PEO-PB) in aqueous solution, which were very clear,[48,49] and it was even possible to distinguish between the corona and the core of the micelle. There, however, the diameter of micelles was larger, 10−20 nm. Accordingly, the appearance of the micelles at a later stage ($t = 6.5$ min) must be a consequence of an increase in the electron density, induced by the penetration of the silicate oligomers into the micelles.[33,50] The EPR study, carried out under the same conditions as the H_3PO_4 reaction, showed that during the first 5 min of the reaction silicate ions with water molecules penetrate into the micelles, which may cause also an increase in their sizes. The reported size of the P123 micelles (for concentration smaller than 8 wt %) at 25 °C is 9−9.6 nm, which is in the same range of the size observed at 22 min (at 50 °C),[51] although a change

in the temperature can cause an increase in the hydrodynamic radius.[52]

The transformation of the spheroidal micelles into TLMs with the progression of the reaction is a consequence of a decrease in the curvature of the micelles induced by the interaction with the silicate oligomers.[53,54] Hence, the silicate adsorption and polymerization decrease the effective volume of the polar region, the PEO part of the polymer. This phenomenon was also observed when salt/electrolytes were added to micellar solutions of Pluronic block-copolymers.[17,55] There it was noted that the presence of the electrolytes increased the hydrophobicity of the Pluronic molecules, which in turn reduced the critical micelle concentration. Similarly, the addition of electrolytes decreased the temperature of the sphere-to-cylinder transition.[55] This is consistent with the EPR/ESEEM results, which showed that, during this growth time, the polarity of the core/corona interface and its water content decreased.[33] The reduction in water content was sensed primarily during the first 60 min of the reaction by a hydrophobic spin probe located in the hydrophobic core of

(48) Zheng, Y.; Won, Y. Y.; Bates, F. S.; Davis, H. T.; Scriven, L. E.; Talmon, Y. *J. Phys. Chem. B* **1999**, *103*, 10331.
(49) Won, Y.-Y.; Brannan, A. K.; Bates, F. S. *J. Phys. Chem. B* **2002**, *106*, 3354.
(50) Boissière, C.; Larbot, A.; Bourgaux, C.; Prouzet, E.; Bunton, C. A. *Chem. Mater.* **2001**, *13*, 3580.
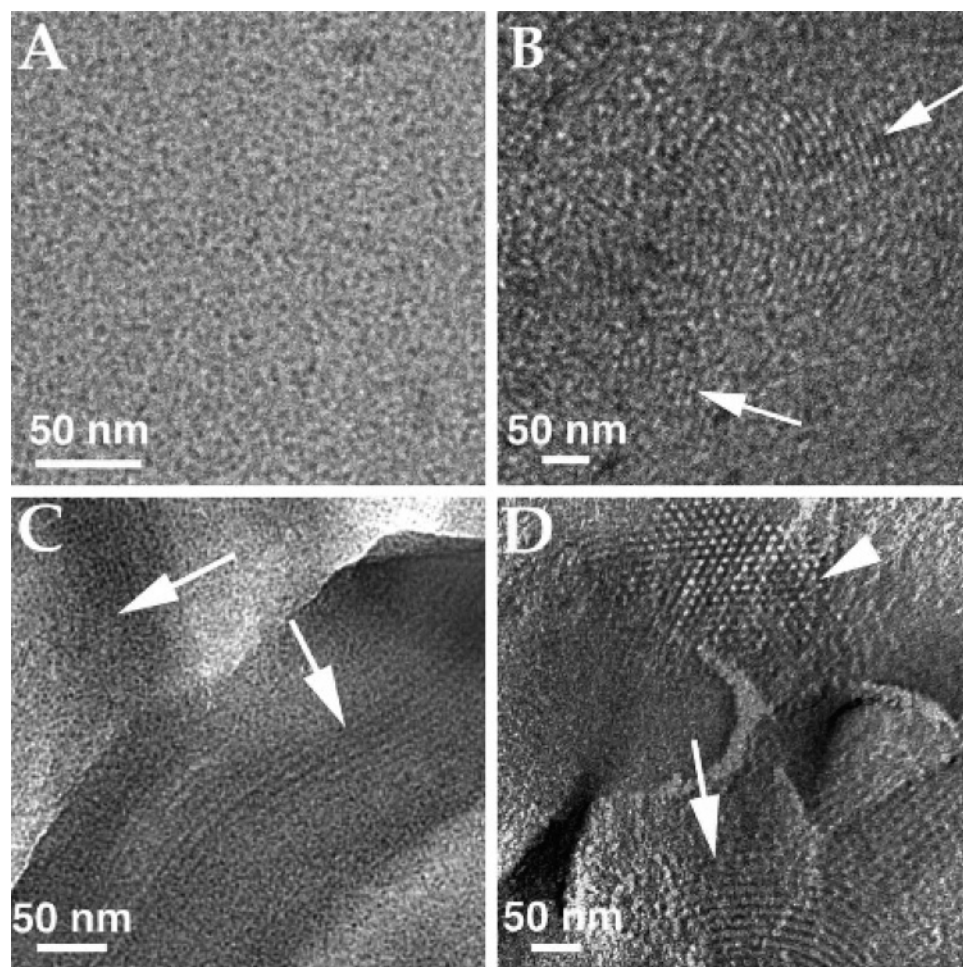
(51) Nolan, S. L.; Phillips, R. J.; Cotts, P. M.; Dungan, S. R. *J. Colloid Interface Sci.* **1997**, *191*, 291.
(52) Mortensen, K. *J. Phys.: Condens. Matter* **1996**, *8*, A103.
(53) Regev, O. *Langmuir* **1996**, 12, 4940.
(54) Israelchvili, J.; Mitchell, D. J.; Ninham, B. *Intermolecular and Surfaces Forces*; Academic Press: 1985.
(55) Booth, C.; Attwood, D. *Macromol. Rapid Commun.* **2000**, *21*, 501.

Figure 6. Cryo-TEM images of the SBA-15 reaction in HCl vetrified at 35 °C. (A) $t = 5$ min 13 sec. (B) $t = 14$ h 5 min. Arrows show the TLMs. (C) Freeze−fracture replication of the same system for $t = 16$ min 27 sec where arrows point to TLMs. (D) Same $t = 21$ min 42 sec. Note the hexagonal arrangement of the micelles seen along their long axes (arrowhead) and the view perpendicular to the long axis (arrow).

the micelle. Spin probes located within the corona sensed such changes later, during $t = 60-120$ min. Hence we conclude that this reduction in water content is a consequence of the silicate oligomerization within the corona of the micelles, which further increases the hydrophobic character of the core/corona interface, thereby reducing the effective volume of the corona and decreasing the curvature. These changes may be associated with a contraction of the corona that leads to the reduction of the diameter of the TLMs observed in the cryo-TEM experiments. The TLMs continue to grow with time, and their structure becomes less flexible and straighter. Furthermore, aggregates of long threads showed up to 40 min, after which no more direct imaging cryo-TEM measurements could be carried out. Interestingly, the EPR results did no show any special feature at 40 min, although this is the time at which a precipitate is observed.

The in situ CW EPR spectra, using spin probes located in the corona, show continuous changes in the polarity up to $t \approx 120$ min.[32] This suggests that the precipitation is a consequence of the increasing size of the TLMs and their aggregation, while the process responsible for the water expulsion and polarity reduction continues. These can occur either within the precipitate or in structures that are still in solution and precipitate later. The EPR results also showed that the P123 molecules within the TLMs remain highly mobile (on the EPR time scale), even after precipitation, until drying takes place. SAXS measurements

done on a dried solid after 2 h of reaction[32] showed a hexagonal order, whereas this hexagonal structure was clearly observed by FFR after 2 h 50 min of reaction, although some structure was also evident after 2 h. This suggests that the drying process promotes the formation of the hexagonal structure. Finally, the observed phase separation into a dilute phase of spheroidal micelles coexisting with a phase of micelles that develops into TLMs has not been resolved by EPR.

Figure 7 presents a schematic model that summarizes the evolution of microstructures in the formation of SBA-15, based on results from this study and from the EPR studies. Initially, only spheroidal micelles are present in the reaction mixture, silicate oligomers penetrate into the core−corona interface of the micelle, causing a decrease in the curvature of the corona region, and then TLMs appeared. These TLMs become less flexible and straighter, with the progression of the condensation of silicate oligomers in the corona region. At $t = 40$ min the number of these flocs increases, leading to precipitation, and in a later stage the hexagonal structure is formed ($t > 2$ h).

Comparison with Other in Situ Studies on SBA-15. The direct imaging cryo-TEM and FFR results show that the transition to the hexagonal order takes place after precipitation. In situ SAXS/XRD measurements that were carried out on SBA-15 prepared with P123, TMOS, and HCl at 35 °C[35] showed that, after the solution turned turbid, at 25 min, a sharp transition
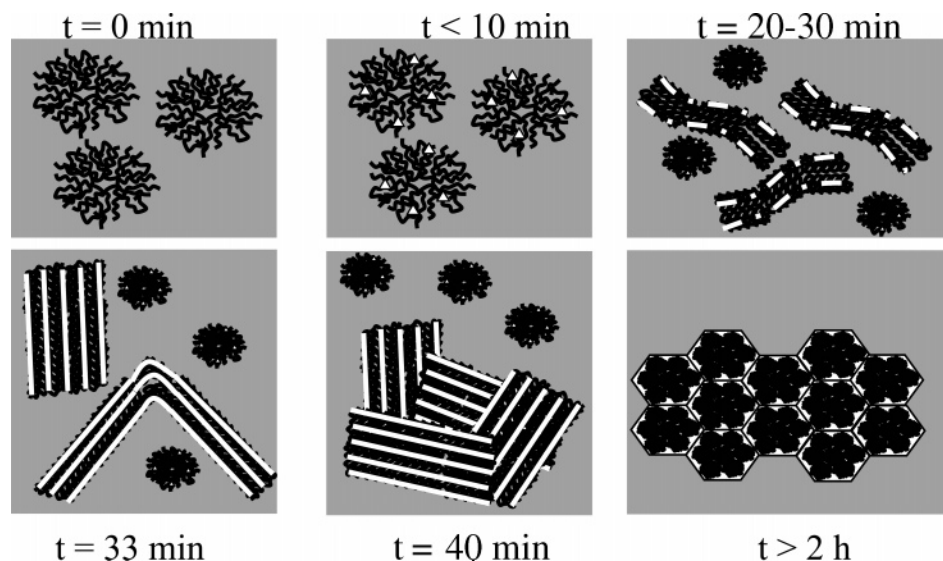
Figure 7. A schematic model describing the evolution of microstructures in the formation of SBA-15. The white dots/lines represent silicate oligomers. The time scale corresponds to the H_3PO_4 reaction.

from spheroidal micelles to a 2D hexagonal phase occurred at $t = 40$ min. In a similar reaction mixture, where TEOS is used instead of TMOS, this transition occurred at 50 min due to a slower hydrolysis of TEOS. The analysis of the broad peak observed between 15 and 40 min, prior to the appearance of the 2D hexagonal phase, showed the presence of spheroidal micelles with a constant core radius of 4.5 nm and a total radius of 7.0 nm. The authors did try to fit the scattering data to finite cylindrical micelles, but failed to obtain a good fit. These results, however, have been challenged by a recent publication by Khodakov et al.[56] who have also studied the initial stages of the SBA-15 synthesis in the presence of HCl and TEOS by SAXS. There, however, the authors succeeded in fitting their data with cylindrical micelles. Individual cylindrical micelles were present between 5 and 20 min after the addition of TEOS, where in the first 5 min of the reaction only spheroidal micelles appear. At 20 min, precipitation started, and at 25 min, a hexagonal structure appeared. While the mechanism proposed by the first in situ SAXS report is inconsistent with the mechanism we proposed on the basis of the cryo-TEM and FFR results, the results of the second study are in full agreement. It is clear from this SAXS/XRD and our cryo-TEM experiments that the synthesis conditions affect the rate of the reaction. When HCl is used, the reaction rate is significantly faster, making it difficult to "catch" individual TLMs, which were very clear in the slower synthesis with H_3PO_4. Nevertheless, although the reaction rate with HCl is faster, it was still possible to detect the presence of TLMs, before precipitation, showing that they are the driving force for the formation of the hexagonal structure.

In situ ^{1}H NMR measurements[26] were also carried out on the reaction mixture of SBA-15, employing the same reaction conditions used in the SAXS/XRD studies. The signal observed was that of the PO methyl group, and a sharp increase in the line width was observed between 23 and 24 min, just before the appearance of the turbidity. No special event was observed in the time evolution of the NMR spectrum that can be associated with the transition to the hexagonal phase at 40 min.

(56) Khodakov, A. Y.; Zholobenko, V. L.; Impéror-Clerc, M.; Durand, D. *J. Phys. Chem. B* **2005**, *109*, 22780.

TEM measurements were carried out as well in that case, though under somewhat different conditions. The reaction was quenched by dilution at a particular time, and then the samples were filtered and dried. The TEM micrographs showed that, after precipitation (25 min), elongated micelles were detected after 40 min and only after 55 min their hexagonal packing became evident. The model the authors constructed based on the NMR and TEM results is that the silica adsorption and polymerization occur within the corona, reducing the interaction between micelles, thereby producing flocs of a number of spheroidal micelles. These flocs then further associate, increasing the particle size and leading to precipitation. Then micelle−micelle coalescence takes place within the flocs to form the cylindrical micelles and hexagonal order. Again, this mechanism is different from the one portrayed by the direct imaging cryo-TEM, where the elongation of the micelles and formation of TLMs are observed in solution prior to precipitation. We note, however, that cryo-TEM stands a better chance of preserving the original structure of the aggregates in solution compared to the above TEM sample preparation.

The formation of SBA-15 was also studied by exploring the morphology of the particles formed after precipitation using scanning electron microscopy (SEM).[36] The reaction conditions chosen were those that yield a 100% rodlike morphology, prepared with HCl and TEOS with the addition of KCl at 38 °C. Under these conditions precipitation appeared after 15 min. The solid was separated by filtration and washed with water and ethanol to remove any remaining surfactant. Spheres of 100 nm diameters were observed 5 min after precipitation, and TEM showed that they had a wormlike mesoporous structure, indicating that the hexagonal structure developed after precipitation. Here, however, one has to take into account that the filtering and drying may intervene with the natural progression of the reaction.

To summarize, all these studies, including the present cryo-TEM findings show that in SBA-15, the precipitate consists of aggregates of surfactant-silica micelles, not yet organized into a clear hexagonal structure. There is disagreement with respect to evolution of the micelle shapes as a consequence of the

interaction with the silicate: while we, and the recent SAXS study,[56] detected elongation of the micelles and the formation of bundles, yet another study reported no changes in the micelle shape, just their condensation.[35] This difference is significant, as it stems from the effect of the silicate adsorption and oligomerization on the curvature of the micelles.

In a recent theoretical study,[57] mean-field theory was used to obtain the thermodynamic equilibrium phase diagram of the surfactant–silicate composite, assuming that the amount of adsorbed silicate is a parameter that determines the spontaneous curvature and the effective surfactant–surfactant interaction. The phase diagram, which depends on the concentration of surfactant and adsorbed silicate, shows that the first transformation to take place is from spheroidal to elongated micelles, consistent with our results. Then, depending on the relative ratio between the adsorbed silicate and the surfactant, a nematic, hexagonal, or disordered network can be obtained.

Comparison with MCM-41. The formation of MCM-41, obtained with a charged surfactant is much faster than that of SBA-15. In situ XRD has shown that, under the conditions of high pH and with TEOS as the silica source, the hexagonal structure developed within 3 min.[34] Therefore, the solution microstructures were probed by cryo-TEM only at a single time point, 3 min after the TEOS addition, where ordered clusters of elongated micelles (with 5 nm micelle-to-micelle average distance) were observed.[53] Some other features observed in the micrographs were interpreted as bundles of elongated micelles wrapped in by a silica film. The same structures were observed in micrographs obtained at 10 and 15 min. Hence, it seems that the reaction is too fast for the observation of the evolution of the solution microstructure.

Cryo-TEM experiments were also carried out on an MCM-41 prepared with a mixture of an anionic surfactant, decanoate, and with a conventional cetyltrimetheylammonium bromide (CTAB) template.[40] This addition led to a 2D hexagonal-to-lamellar phase transition. Here, after 85 s threadlike surfactant–silicate micelles, with occasional junctions, were observed. At this stage no ordering was detected by SAXS/XRD. Later, at 210 s, the threadlike micelles developed into a vesicular structure mixed with a lamellar structure, while the SAXS/XRD showed the presence of a mixture of hexagonal and lamellar phases. An in situ SAXS/XRD study was also carried out on

an ordered hexagonal mesophase formed from a bridged organo-silane.[58] The micelles remained spheroidal until the nucleation and growth of the hexagonal phase. Again, a different behavior than that was observed by the cryo-TEM measurements on SBA-15. In this case, however, one has to take into account that the reaction was carried out at a high temperature, 95 °C, the silica source is different, and the hydrolysis is significantly slower.

Conclusions

The evolution of the micellar structures during the formation of SBA-15 was followed by direct imaging cryo-TEM and freeze–fracture replication cryo-TEM. A continuous transformation from spheroidal micelles, into threadlike micelles, which become longer and stiffer, followed by the formation of bundles with the dimensions similar to those found in the final material, was observed. The network grows through equilibrium with a phase of diluted spheroidal micelles, which transformed with time into the viscous phase. The evolution of the shapes implies that silicate precursors adsorbed and polymerized at the hydrophilic micellar interface, thereby reducing its curvature. This is consistent with the EPR results, which showed that, during TLMs' growth time, the polarity and water content of the core/corona interface decreases. The ordered hexagonal structure was observed by freeze–fracture replication. The same evolution of micellar structure in solution was observed for reactions carried out with HCl and H_3PO_4, but the rates were different.

(57) Gov, N.; Boruknov, I.; Goldfarb, D. *Langmuir* **2006**, *22*, 605.

(58) Morell, J.; Teixeira, C. V.; Cornelius, M.; Rebbin, V.; Teimann, M.; Amenitsch, H.; Fröba, M.; Lindén, M. *Chem. Mater.* **2004**, *16*, 5564.